

Short communication

Characteristics of $\text{Ba}_{0.5}\text{Sr}_{0.5}\text{Co}_{0.8}\text{Fe}_{0.2}\text{O}_{3-\delta}$ – $\text{La}_{0.9}\text{Sr}_{0.1}\text{Ga}_{0.8}\text{Mg}_{0.2}\text{O}_{3-\delta}$ composite cathode for solid oxide fuel cell

Bangwu Liu^a, Yue Zhang^{a,b,*}, Limin Zhang^a

^a Department of Materials Physics, University of Science and Technology Beijing, Beijing 100083, People's Republic of China

^b Key Laboratory of New Energy Materials and Technologies, University of Science and Technology Beijing, Beijing 100083, People's Republic of China

Received 5 July 2007; received in revised form 22 September 2007; accepted 24 September 2007

Available online 2 October 2007

Abstract

$\text{Ba}_{0.5}\text{Sr}_{0.5}\text{Co}_{0.8}\text{Fe}_{0.2}\text{O}_{3-\delta}$ – $\text{La}_{0.9}\text{Sr}_{0.1}\text{Ga}_{0.8}\text{Mg}_{0.2}\text{O}_{3-\delta}$ composite cathodes are prepared successfully using combustion synthesis method. Microstructure, chemical compatibility and electrochemical performance have been investigated and analyzed in detail. SEM micrographs show that a structure with porosity and well-necked particles forms after sintering at 1000 °C in the composites. Grain growth is suppressed by addition of $\text{La}_{0.9}\text{Sr}_{0.1}\text{Ga}_{0.8}\text{Mg}_{0.2}\text{O}_{3-\delta}$ phase and grain sizes decrease with increasing weight percent of $\text{La}_{0.9}\text{Sr}_{0.1}\text{Ga}_{0.8}\text{Mg}_{0.2}\text{O}_{3-\delta}$ phase in the composites. Phase analysis demonstrates that chemical compatibility between $\text{Ba}_{0.5}\text{Sr}_{0.5}\text{Co}_{0.8}\text{Fe}_{0.2}\text{O}_{3-\delta}$ and $\text{La}_{0.9}\text{Sr}_{0.1}\text{Ga}_{0.8}\text{Mg}_{0.2}\text{O}_{3-\delta}$ is excellent when the weight percent of $\text{La}_{0.9}\text{Sr}_{0.1}\text{Ga}_{0.8}\text{Mg}_{0.2}\text{O}_{3-\delta}$ in the composite is not more than 40%. Through fitting ac impedance spectra, it is found that the ohmic resistance and polarization resistance decrease with increasing $\text{La}_{0.9}\text{Sr}_{0.1}\text{Ga}_{0.8}\text{Mg}_{0.2}\text{O}_{3-\delta}$ content. The polarization resistance reaches a minimum at about 30 and 40 wt.% $\text{La}_{0.9}\text{Sr}_{0.1}\text{Ga}_{0.8}\text{Mg}_{0.2}\text{O}_{3-\delta}$ in the composite.

© 2007 Elsevier B.V. All rights reserved.

Keywords: $\text{Ba}_{0.5}\text{Sr}_{0.5}\text{Co}_{0.8}\text{Fe}_{0.2}\text{O}_{3-\delta}$; $\text{La}_{0.9}\text{Sr}_{0.1}\text{Ga}_{0.8}\text{Mg}_{0.2}\text{O}_{3-\delta}$; Composite cathode; Solid oxide fuel cell

1. Introduction

Fuel cells have attracted much attention in recent years due to their various advantages such as high energy efficiencies and low pollutant emissions. Except for these advantages, another important one for the solid oxide fuel cell (SOFC) is its fuel flexibility [1]. Not only hydrogen but also various kinds of hydrocarbon can be used as fuel [2]. Conventional SOFC generally operates at 1000 °C, which seriously limits its development. Many efforts attempt to reduce operating temperatures to below 800 °C and develop intermediate temperature solid oxide fuel cell (ITSOFC) [3,4]. In order to improve performance of ITSOFC, a group of new materials have been developed. Sr- and Mg-doped lanthanum gallate ($\text{La}_{1-x}\text{Sr}_x\text{Ga}_{1-y}\text{Mg}_y\text{O}_{3-\delta}$) is a promising electrolyte material, which has high oxygen-ion

conductivity at intermediate temperatures, i.e. approximately 10^{-1} S cm at 800 °C [5,6]. $\text{Ba}_{0.5}\text{Sr}_{0.5}\text{Co}_{0.8}\text{Fe}_{0.2}\text{O}_{3-\delta}$ (BSCF) has been reported by Shao et al. as a novel cathode material for SOFC recently and it shows high electrical conductivity, high oxygen diffusion and good electrochemical performances [7]. Peña-Martínez et al. [8] used $\text{La}_{0.9}\text{Sr}_{0.1}\text{Ga}_{0.8}\text{Mg}_{0.2}\text{O}_{2.85}$ (LSGM) as electrolyte, $\text{Ba}_{0.5}\text{Sr}_{0.5}\text{Co}_{0.8}\text{Fe}_{0.2}\text{O}_{3-\delta}$ as cathode and $\text{La}_{0.75}\text{Sr}_{0.25}\text{Cr}_{0.5}\text{Mn}_{0.5}\text{O}_{3-\delta}$ (LSCM) as anode material to test an intermediate temperature solid oxide fuel cell. Results showed that the use of BSCF material on LSGM seemed to be feasible. To improve the performance of SOFC further, it is necessary to reduce cathode polarization [9,10]. For this purpose, the use of composite cathodes, which compose of electrocatalyst and electrolyte allows enlargement of triple phase boundaries (TPBs) where reaction of oxygen occurs [11]. Many studies have also demonstrated that composite cathodes exhibit much lower overpotentials than single-phase electrodes made of the electrocatalyst alone [12].

In the present study, series of BSCF–LSGM composite cathodes were prepared using combustion synthesis method.

* Corresponding author at: Department of Materials Physics, University of Science and Technology Beijing, Beijing 100083, People's Republic of China. Tel.: +86 10 62333113; fax: +86 10 62332281.

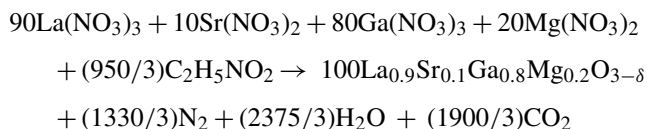
E-mail address: yuezhang@ustb.edu.cn (Y. Zhang).

Chemical compatibility, microstructure and electrochemical performance would be studied and analyzed in detail. These results could lead to a useful guide for designing cathode for ITSOFC based on LSGM electrolyte.

2. Experimental

2.1. Preparation

Powders of $\text{La}_{0.9}\text{Sr}_{0.1}\text{Ga}_{0.8}\text{Mg}_{0.2}\text{O}_{3-\delta}$ were synthesized from the following initial materials: Ga_2O_3 (99.999%), $\text{La}(\text{NO}_3)_3 \cdot 6\text{H}_2\text{O}$ (AR grade), $\text{Mg}(\text{NO}_3)_2$ (AR grade), $\text{Sr}(\text{NO}_3)_2$ (AR grade), and glycine ($\text{H}_2\text{NCH}_2\text{COOH}$, AR grade). Ga_2O_3 was first dissolved into strong HNO_3 and heated to 200–250 °C until the colorless $\text{Ga}(\text{NO}_3)_3$ aqueous solution was obtained. According to the formula of $\text{La}_{0.9}\text{Sr}_{0.1}\text{Ga}_{0.8}\text{Mg}_{0.2}\text{O}_{3-\delta}$, stoichiometric amounts of nitrates of La, Sr, Ga and Mg were mixed in the deionized water. The amount of glycine was determined by propellant chemistry. As the principle of propellant chemistry, the stoichiometric redox reaction can be expressed as follows:



The stoichiometric molar ratio of glycine to oxidant is 1.58:1. Taking into account a little amount of HNO_3 in the nitrates solution, the molar ratio of glycine to oxidant could be raised to 1.7:1. The aqueous solution of nitrates and glycine was heated in a baker, and sufficient water was evaporated until the solution boiled, began to froth and spontaneously burn. The as-synthesized powders were heated at 1000 °C for 2 h to decompose residual reactants and were subsequently furnace cooled to room temperature.

During the course of preparing $\text{Ba}_{0.5}\text{Sr}_{0.5}\text{Co}_{0.8}\text{Fe}_{0.2}\text{O}_{3-\delta}$ powders, $\text{Ba}(\text{NO}_3)_2$ (AR grade), $\text{Sr}(\text{NO}_3)_2$ (AR grade), $\text{Fe}(\text{NO}_3)_3 \cdot 9\text{H}_2\text{O}$ (AR grade), $\text{Co}(\text{NO}_3)_2 \cdot 6\text{H}_2\text{O}$ (AR grade) and

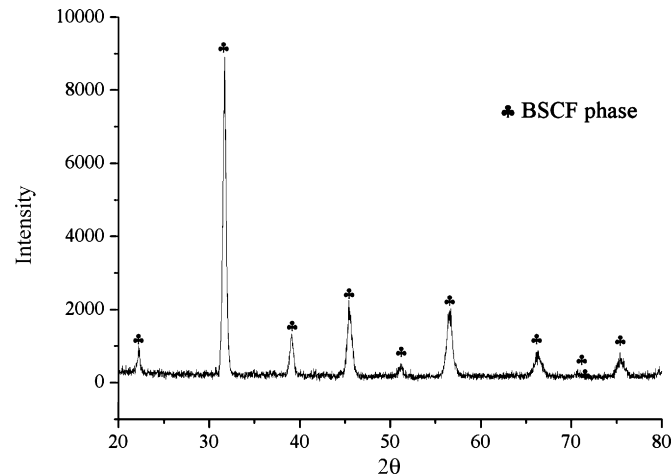
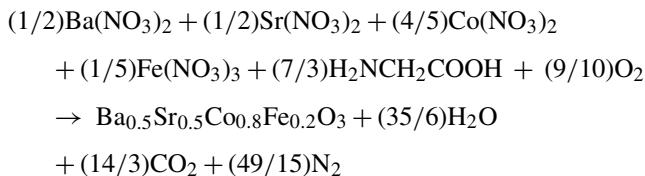


Fig. 2. The XRD pattern of the calcined BSCF powders.

glycine were used as starting materials. According to propellant chemistry, the stoichiometric redox reaction can be expressed as follows:



The stoichiometric molar ratio of glycine to nitrate ions in this reaction is 0.56. The experimental process is similar to that of synthesizing LSGM powders. The as-prepared powders were calcined at 850 °C for 2 h in the air to obtain pure, well-crystallized powders.

The BSCF powders after 850 °C heat treatment were mixed with the as-calcined LSGM powders according to different ratios. The BSCF–LSGM mixture compositions were varied from 0 to 50 wt.% LSGM (and hereafter identified as M0, M10, M20, M30, M40 and M50). These mixtures were ground in the mortar for 10 min, respectively. And then, each mixture was weighed 0.8 g to press pellets under 20 MPa pressure. The pellets

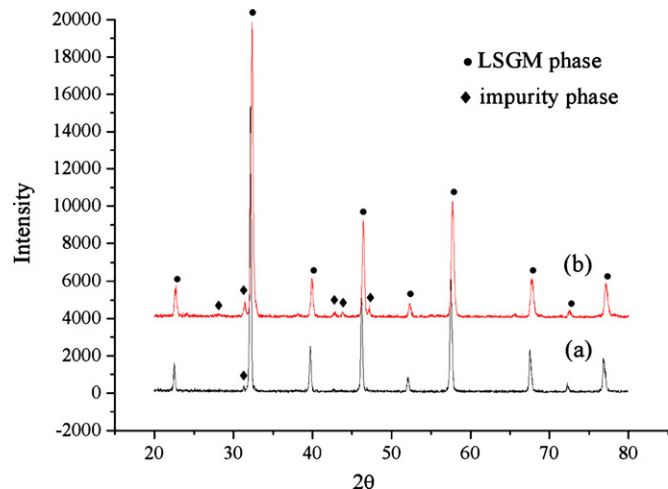


Fig. 1. (a) The XRD pattern of as-prepared LSGM powders and (b) the XRD pattern of LSGM powders calcined at 1000 °C.

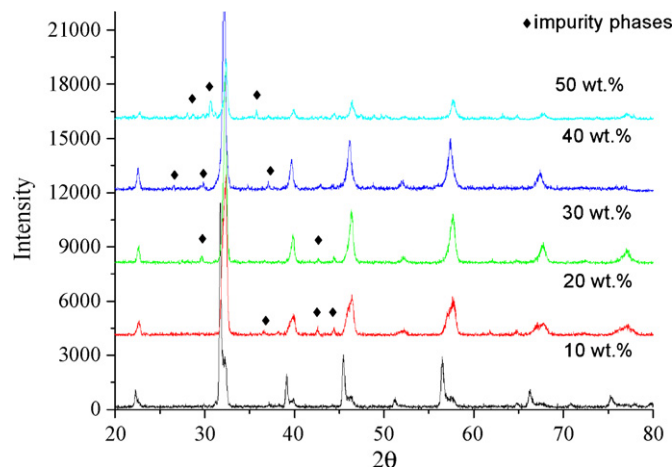


Fig. 3. XRD patterns of the composites with 10, 20, 30, 40, 50 wt.% LSGM.

were sintered for 2 h at 1000 °C in the air, and were subsequently furnace cooled to room temperature.

2.2. Symmetrical fuel cell fabrication

The calcined LSGM powders were sintered for electrolyte pellets at 1250 °C under a pressure of 40 MPa by spark plasma sintering (SPS). Both sides of the pellet are roughed with

240# SiC grit paper and then cleaned by ultrasonic. The electrode slurry is made with desired amount of BSCF and LSGM together with ethylene glycol and ball milled for 20 h. The slurry is painted with brush onto both sides of the LSGM pellet. The cell is first heated upto 500 °C to eliminate the organic binders, and then to 1000 °C for 2 h. After sintering, the symmetrical cell with an area of about 0.5 cm² cathode films was obtained.

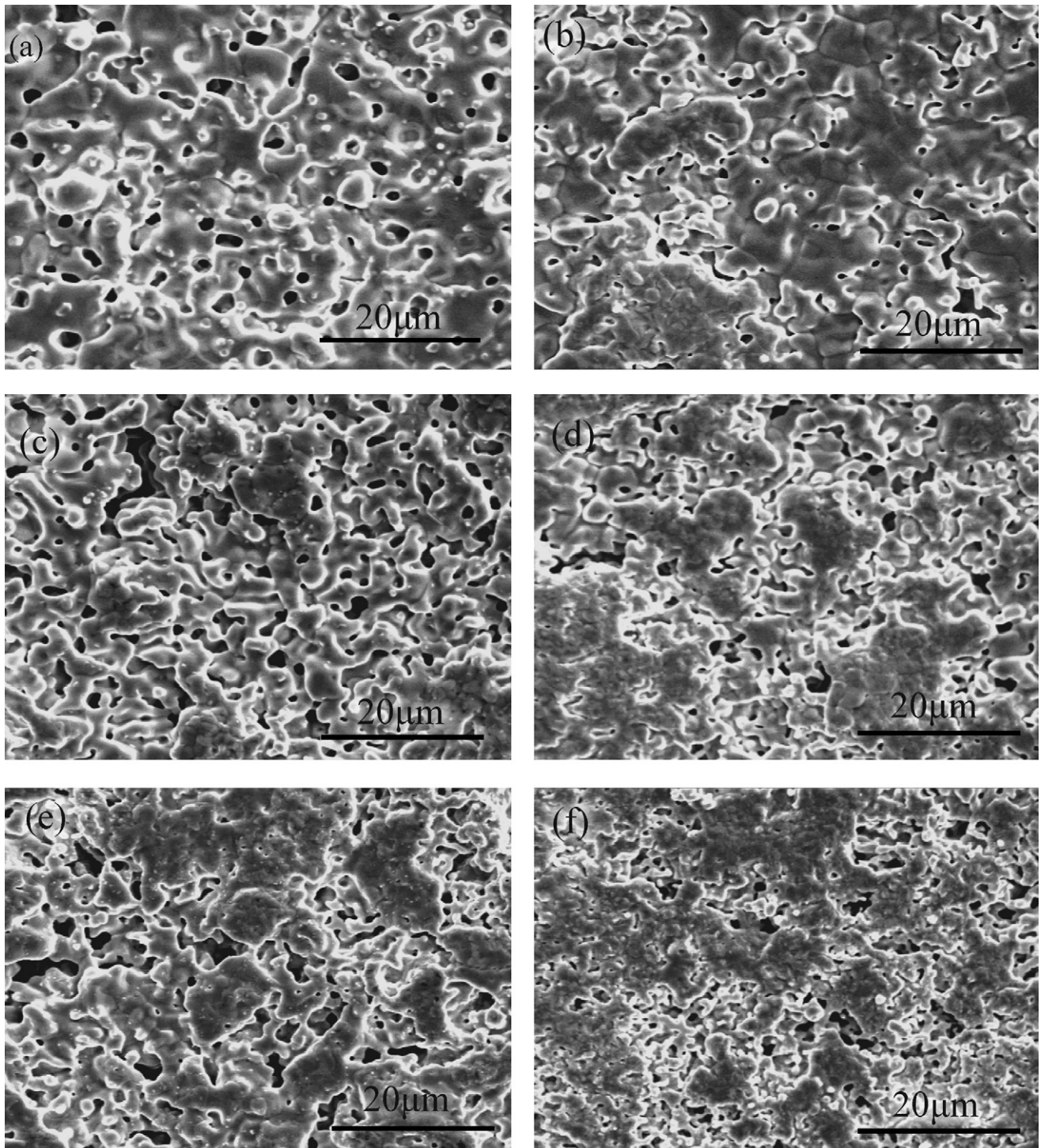


Fig. 4. The microstructure of composites, the contents of LSGM in (a)–(f) are 0, 10, 20, 30, 40 and 50 wt.%, respectively.

2.3. Characterization

X-ray diffraction analysis (XRD) was carried on to identify phase formation and chemical compatibility using Cu K α radi-

ation at a scanning speed of 0.02° per step on a Rigaku Dmax-RB X-ray diffractometer. Morphology observation of the samples after sintering was performed in a Cambridge S-360 scanning electron microscope (SEM). Impedance spectra of composite

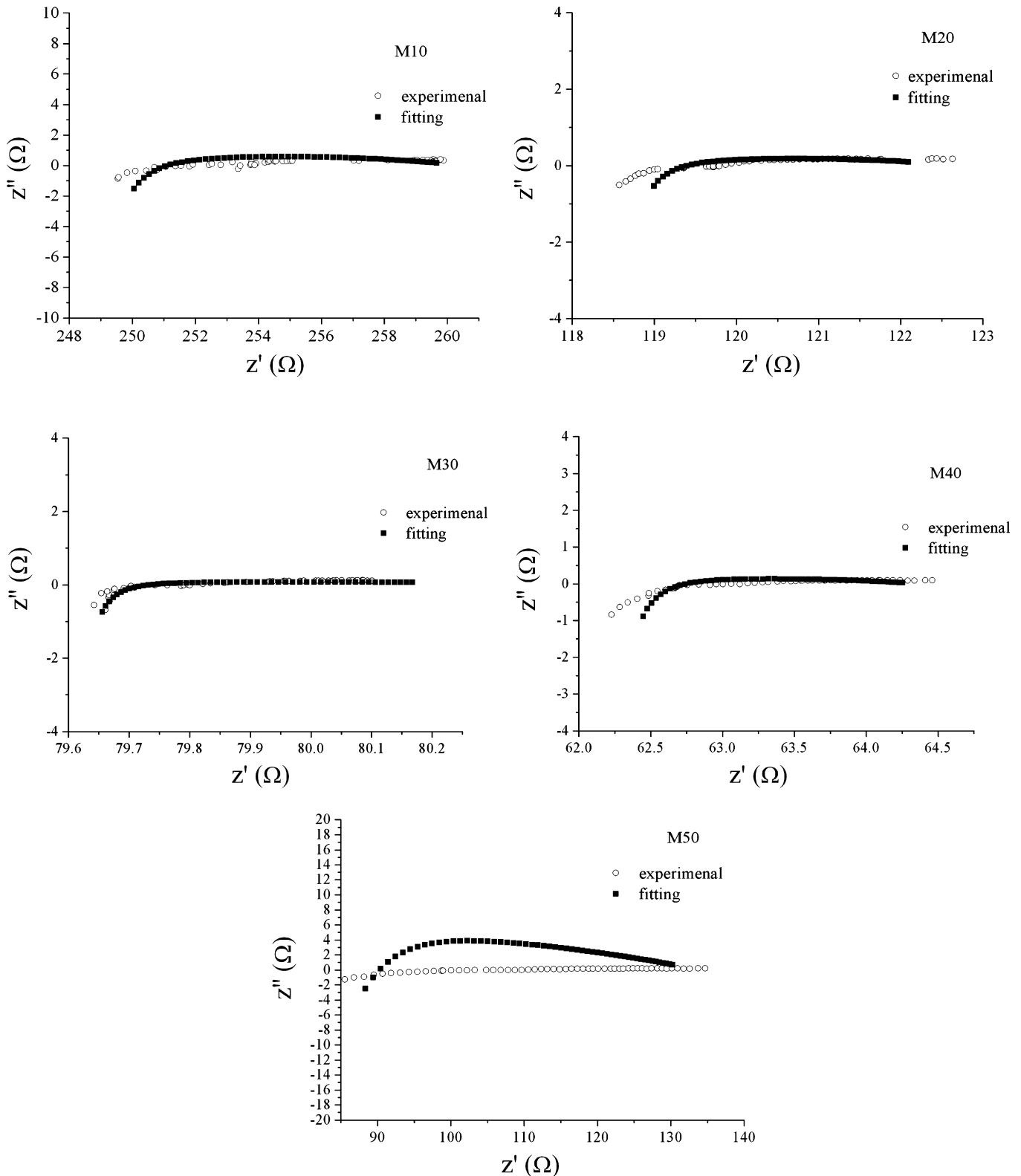


Fig. 5. ac impedance spectra of M10, M20, M30, M40 and M50 at room temperature in the air.

cathode pellets were measured at room temperature while symmetrical cell pellets were measured 500–800 °C in the air by impedance analyzer (Solartron SI 1287). The measuring frequency range was from 0.1 Hz to 1 MHz. A *z*-view 2.0 software was used to fit the impedance data and to calculate the resistances of the samples.

3. Results and discussion

3.1. Phase analysis and chemical compatibility

The XRD pattern of as-prepared LSGM powders is shown in Fig. 1(a). It can be seen that perovskite-type LSGM phase has formed during the combustion process. The amount of impurity phase is so little that the impurity phase becomes almost undetectable in XRD analysis. The crystal structure of $\text{La}_{0.9}\text{Sr}_{0.1}\text{Ga}_{0.8}\text{Mg}_{0.2}\text{O}_{3-\delta}$ has been studied by previous workers elsewhere [13]. The XRD pattern of calcined LSGM powders is shown in Fig. 1(b). The amount of impurity phase increases after calcining at 1000 °C. This may result from the crystal process of the impurity phase, which is present already in the as-prepared sample in poorly crystalline or amorphous condition. The possible impurity phase should be $\text{LaSrGa}_3\text{O}_7$ and/or SrLaGaO_4 .

The XRD pattern of the calcined BSCF powders measured at room temperature is shown in Fig. 2. All the peaks are well indexed as a cubic perovskite structure, with a space group of *Pm3m*. From calculation using XRD data, the lattice parameter for BSCF, *a*, is refined to 0.3992 nm, which is consistent with reported work [14].

XRD patterns of the binary-mixed systems LSGM/BSCF with different weight ratios are shown in Fig. 3. It seems that there appears some impurity phase in the composites due to formation of impurity phase in LSGM phase during sintering at 1000 °C. And the amount of impurity phase increases with increasing weight percent of LSGM. This is consistent with above analysis. It also seems that chemical compatibility between BSCF and LSGM is excellent when the weight percent of LSGM in the composite is not more than 40%. In the sample M50, BSCF and LSGM seem to react with each other.

3.2. Microstructure

SEM micrographs of composite cathode pellets can be seen from Fig. 4. After sintering at 1000 °C, a structure with porosity and well-necked particles forms. Non-uniform aggregates of LSGM particles are dispersed into the BSCF matrix. This indicates that grinding cannot break up the aggregates of LSGM particles. In order to break up the aggregates and mix BSCF particles with LSGM particles uniformly, ball milling should

Table 1

The fitting results of ac impedance spectra measured at the room temperature

Composites	L (H)	R1 (Ω)	R2 (Ω)	CPE-T (F)	CPE-P (angle [*])
M10	2.5196E-5	247.1	15.9	0.01973	0.21691
M20	1.3237E-5	117.5	6.295	0.066779	0.19634
M30	7.8203E-6	79.51	1.055	0.5615	0.20228
M40	9.5159E-6	61.72	3.077	0.079993	0.22056
M50	2.3083E-5	82.91	46.51	0.0013732	0.35552

* The angle of CPE-P is measured as: 1 = 90°, 0.5 = 45°.

be employed. From SEM micrographs, it can also be seen that grain sizes decrease with increasing weight percent of LSGM phase in the composites. LSGM has a low sintering activity compared with BSCF. In order to sinter LSGM, it requires a high temperature (higher than 1400 °C) and a long time (longer than 6 h). When the composite pellets are sintered at 1000 °C for 2 h, LSGM particles or aggregates can suppress grain growth.

3.3. Impedance spectra

Fig. 5 shows ac impedance spectra of composites with different compositions measured at room temperature in the air. They display an inductive tail at high frequencies and one depressed arc at medium–low frequencies. The impedance spectra are successfully fitted by equivalent circuit as shown in Fig. 6. Here L represents the inductance caused by the device and the connect leads, and R1 is the ohmic resistance of the composites and connect leads. The remaining components represent the total polarization resistance (given by the difference between the real-axis intercepts of the impedance spectrum), corresponding to charge transfer and diffusion or adsorption processes. CPE represents a constant phase element consisting of a CPE-T, which is related to the relaxation capacitance, and a CPE-P which reflects the displacement of the center of the arc from the real axis [15]. The fitting results can be seen in Table 1. From these fitting results, it is concluded that the addition of LSGM into BSCF has a significant effect on the ohmic and polarization resistances. The ohmic resistance and polarization resistance decrease with increasing LSGM content. The only exception is M50, where polarization resistance increases abruptly. This enhancement of performance is explained by considering that introducing the ionic conductor particles into the electrode structure increases the three-phase-boundary length, as the electrochemically active area extends into the electrode's bulk. The polarization resistance reaches a minimum at about 30 and 40 wt.% LSGM in the composite. This is reasonably consistent with predictions based on the effective medium percolation theory (EMPT) [15]. According to EMPT model, 30% porosity will lead to 40% optimum volume fraction electrolyte in electrode materials. The abrupt increase of polarization resistance in M50 probably can be explained from three points. Firstly, the increase LSGM content to more than 50% will lead to a decrease in continuity of BSCF in the composite. This can also explain why M50 have an abrupt increase in ohmic resistance, which is associated with mixed conducting BSCF phase. Secondly, the sintering activity of LSGM is rather low. Under this sintering conditions,

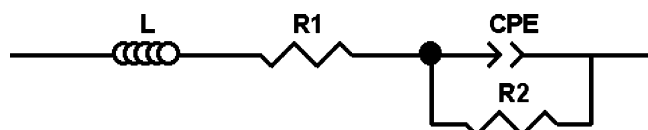


Fig. 6. Equivalent circuit used to fit ac impedance spectra.

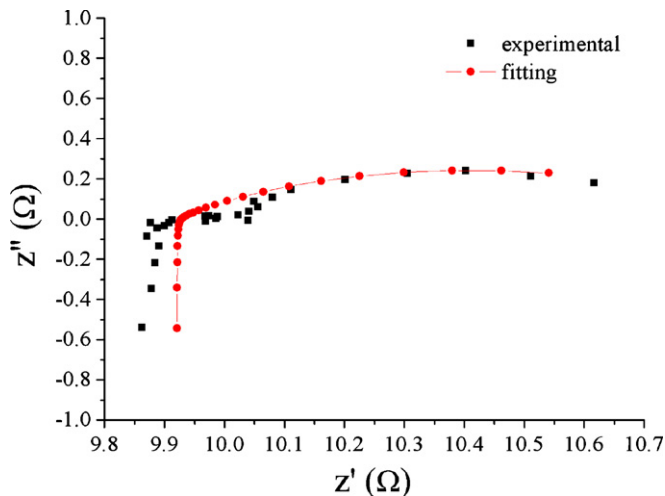


Fig. 7. ac impedance spectra of M0 measured at 800 °C.

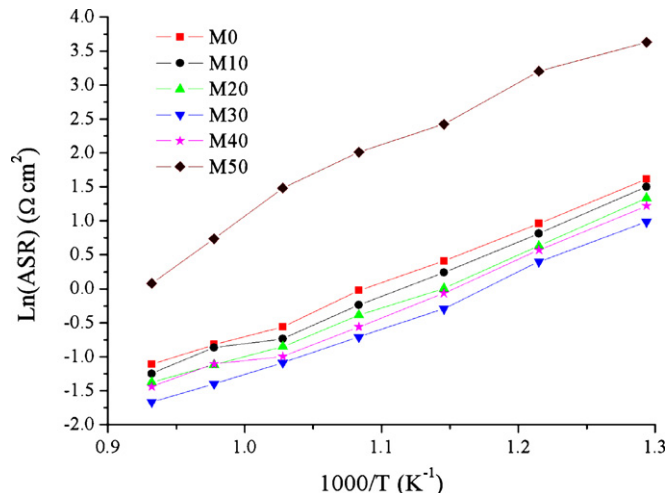


Fig. 9. Ln(ASR) as a function of temperature.

increasing LSGM content to more than 50 wt.% will significantly influence microstructure of composite. Low sintering temperature results in a poor contact between LSGM and LSGM particles. Increasing LSGM content to more than 50 wt.% will also decrease triple phase boundaries. Thirdly, LSGM and BSCF may react with each other when the LSGM content is 50 wt.%. This can be confirmed from XRD results.

The typical ac impedance spectra of symmetric fuel cell measured at 800 °C in the air can be found in Fig. 7 together with the fitting curve. It also can be successfully fitted by equivalent circuit in Fig. 6, where R2 represents resistance at the cathode/electrolyte interface ($R_{\text{interface}}$). The cathode area specific resistance (ASR) can be deduced from the relation: $\text{ASR} = R_{\text{interface}} \times \text{surface area} / 2$. The ASRs for different compositions as function of temperature can be seen from Fig. 8. The ASRs of all the samples are very low, which demonstrates that BSCF is a suitable cathode material for the LSGM electrolyte. However, M50 is exception and its ASR is obviously higher than that of other compositions. This may be due to the poor contact interface between composite and electrolyte, which

results from low sintering activity of LSGM. The ASRs of composites are similar to that of pure BSCF cathode and reach a minimum, $0.189 \Omega \text{ cm}^2$ at 800 °C. Arrhenius plots of ASR of all the samples are plotted in Fig. 9. The activation energies calculated from Arrhenius plots are 126.66, 125.68, 124.7, 123.16, 122.88 and $161.72 \text{ kJ mol}^{-1}$ for M0, M10, M20, M30, M40 and M50, respectively.

It is widely established that the cathode polarization resistance is closely related to the charge transfer and the adsorption/dissociation of oxygen (oxygen reduction reaction, ORR), and the transport speed of oxide ions through the cathode bulk and across the cathode/electrolyte interface. Also it is reported that the ionic conductivity of BSCF is higher than that of LSGM. Hence, it can be inferred that addition of LSGM into BSCF does not increase the transport speed of oxide ions through the cathode bulk and across the cathode/electrolyte interface. However, addition of LSGM into BSCF increases triple phase boundaries where oxygen reduction reaction occurs, resulting a decrease in polarization resistance. This can explain why ASR of composites does not improve obviously compared to BSCF cathode.

4. Conclusions

BSCF–LSGM composite cathodes were prepared successfully using combustion synthesis method. After sintering at 1000 °C, a structure with porosity and well-necked particles forms in the composites. Grain growth is retained by addition of LSGM phase and grain sizes decrease with increasing weight percent of LSGM phase in the composites. Phase analysis shows that chemical compatibility between BSCF and LSGM is excellent when the weight percent of LSGM in the composite is not more than 40%. In the sample M50, BSCF and LSGM react with each other strongly. Through fitting ac impedance spectra, it is concluded that the addition of LSGM to BSCF has a significant effect on the ohmic and polarization resistances. The ohmic resistance and polarization resistance decrease with increasing LSGM content. Compared to BSCF cathode, ASRs of composites do not improve obviously. However, the polar-

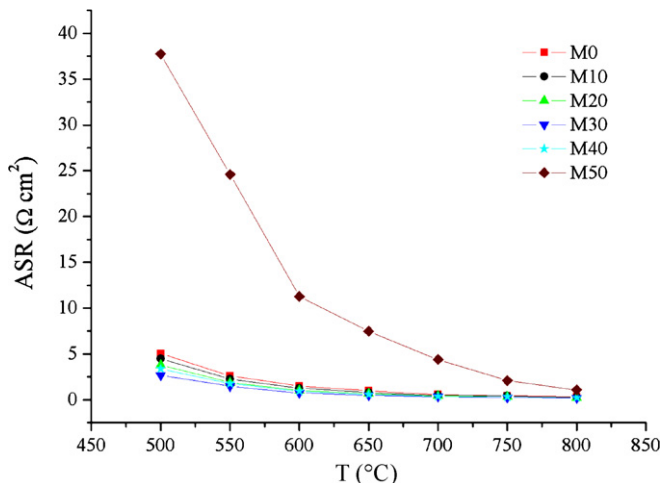


Fig. 8. ASR as a function of temperature.

ization resistance of cathode bulk reaches a minimum at about 30 and 40 wt.% LSGM in BSCF. The activation energies are very low, which demonstrates that BSCF is a suitable cathode material for LSGM electrolyte.

Acknowledgements

This work was supported by National Basic Research Program of China (No. 2007CB936201), the National High Technology Research and Development Program of China (No. 2006AA03Z351), and the Major Project of International Cooperation and Exchanges (Nos. 50620120439, 2006DFB51000).

References

- [1] H. Ishikawa, M. Enoki, T. Ishihara, T. Akiyama, J. Alloys Compd. 430 (2007) 246–251.
- [2] M. Oishi, K. Yashiro, J.-O. Hong, Y. Nigara, T. Kawada, J. Mizusaki, Solid State Ionics 178 (2007) 307–312.
- [3] B.C.H. Steele, A. Heinzl, Nature 414 (2001) 345–352.
- [4] N.P. Brandon, S. Skinner, B.C.H. Steele, Annu. Rev. Mater. Res. 33 (2003) 183–213.
- [5] T. Ishihara, H. Matsuda, Y. Takita, J. Am. Chem. Soc. 116 (1994) 3801–3803.
- [6] C.M. Giovanni Dotelli, R. Mari, R. Ruffo, I. Pelosato, S. Natali, Solid State Ionics 177 (2006) 1991–1996.
- [7] Z. Shao, S.M. Haile, Nature 431 (2004) 170–173.
- [8] J. Peña-Martínez, D. Marrero-López, J.C. Ruiz-Morales, B.E. Buegler, P. Núñez, L.J. Gauckler, Solid State Ionics 177 (2006) 2143–2147.
- [9] C.-C.T. Yang, W.-C.J. Wei, A. Roosen, Mater. Chem. Phys. 81 (2003) 134–142.
- [10] E. Perry Murray, M.J. Sever, S.A. Barnett, Solid State Ionics 148 (2002) 27–34.
- [11] A. Hagiwara, N. Hobar, K. Takizawa, K. Sato, H. Abe, M. Naito, Solid State Ionics 177 (2006) 2967–2977.
- [12] J. Deseure, Y. Bultel, L. Dessemond, E. Siebert, Electrochim. Acta 50 (2005) 2037–2046.
- [13] P. Datta, P. Majewski, F. Aldinger, J. Alloys Compd. 438 (2007) 232–237.
- [14] S. McIntosh, J.F. Vente, W.G. Haije, D.H.A. Blank, H.J.M. Bouwmeester, Chem. Mater. 18 (2006) 2187–2193.
- [15] H. Zhao, L. Huo, L. Sun, L. Yu, S. Gao, J. Zhao, Mater. Chem. Phys. 88 (2004) 160–166.